Turkish Journal of Electrical Engineering & Computer Sciences

http://journals.tubitak.gov.tr/elektrik/

Research Article

Turk J Elec Eng & Comp Sci
(2018) 26: 1638 – 1650

doi:10.3906/elk-1607-41

Diagnosis of reverse osmosis desalination water system using bond graph approach

Abderrahmene SELLAMI, Dhia MZOUGHI*, Abdelkader MAMI
Application Laboratory of Energy Efficiency and Renewable Energies (LAPER), Faculty of Sciences of Tunis, Tunis El Manar University, Tunis, Tunisia

Received: 02.07.2016 • **Accepted/Published Online:** 21.09.2017 • **Final Version:** 30.05.2018

Abstract: Industrial systems have become quite complicated. It is therefore necessary to look for a reliable supervision system to properly treat the information and make the appropriate decision to stop the system or leave it in operation. Supervision of automated systems goes to the heart of the matter. This paper concerns the design of a new methodology for diagnosis based on bond graph modeling. We apply a diagnostic method by Luenberger observer using the bond graph approach on a desalination unit. Tests are carried out on the water input pressure delivered by the pump and the output flow rates of the reverse osmosis. This method will allow us to test normal and failure operations of an industrial system. The roles of diagnostic systems for industrial processes consist of detecting and locating faults, also called residues, that will affect these processes. In order to be effective, the diagnostic system should be robust for residue analysis and insensitive to false alarms. In this context, the development of the proposed method is described from the step of modeling to the step of generation of certain residues.

Key words: Diagnosis, bond graph, Luenberger observer, reverse osmosis desalination system

1. Introduction

Recently used supervision methods for industrial systems are based on very slow approaches and it is necessary to look for fast supervision methods based on automatic observing systems with sensors. By means of these supervision methods, not only can we save time in finding faults but we can also save money by employing only one sensor per residue. The basic idea in performing surveillance or diagnostics of systems is to compare the actual system behavior with the behavior predicted by a proper functioning model. If the model operates properly, i.e. under normal operation (no faults), then the residues that reflect the comparison between the outputs of the system and the observer are zero; otherwise, in abnormal conditions, residues will be nonzero.

Engineering sciences rely heavily on estimates of system states and observer diagnosis is used for estimating actuator and sensor faults [1–4]. Usually industrial systems are governed by a number of physical phenomena and various technology components; for this, the bond graph approach based on energy analysis and multiphysics is well suited. The bond graph modeling tool was defined by Paynter [5]. This energy approach allows the highlighting of analogies between different areas of physics (mechanics, electricity, hydraulics, thermodynamics, acoustics, etc.) and representation of multidisciplinary physical systems in a homogeneous form [6–11].

A method for generating analytical redundancy relations from a linear monoenergy bond graph model

*Correspondence: dhia.mzoughi@gmail.com

by following the causal paths was studied in [12]. At the junction structure level (junctions 0, 1, TF, and GY), several relations between different flows and efforts can be established. The method is interesting but remains limited and complicated in the presence of a large system as well as lacking instrumentation for most parts of real systems, leaving the state inaccessible to measurement; this lack imposes the synthesis of observers whose role is to estimate all or part of the state. Structural analysis can be performed directly from the bond graph model [13]. It is possible to also determine the model order, the rank of the state matrix, the observability, and the controllability conditions of an industrial system. The bond graph approach was used in the synthesis of the Luenberger observer in the case of linear systems [14–21].

In this paper, the bond graph tool is used both to construct the observer's model, namely the construction of a full-order observer, and to calculate the gains of the observer; a diagnostic technique of linear systems with the Luenberger observer using bond graphs will be proposed. The paper is structured as follows: Section 1 has provided a general overview of diagnosis by proportional observer using the bond graph model. Section 2 presents the reverse osmosis test bench and its word bond graph (it gathers the energy source, an adaptation module, and the desalination unit). The bond graph model of reverse osmosis is given in Section 3. The last section presents the diagnosis of the reverse osmosis desalination unit.

2. Diagnosis by proportional observer using the bond graph model

The observer provides an estimate of the system state from its model and measurements of its inputs and outputs. The observer conventionally used in linear systems is called a proportional gain or Luenberger observer [22–24]. A continuous system, described by the state equation, Eq. (1), using the bond graph model is shown in Figure 1, which includes the basic elements of bond graph approach to a system. These basic elements are classified as three passive components (dissipative element R, inertial element I, and storage element C), two active elements (effort source Se and flow source Sf), four junctions (1-junction and 0-junction, which respectively correspond to series connections and parallel connections, while the transformer TF and the gyrator GY are used to go from one field of physics to another).

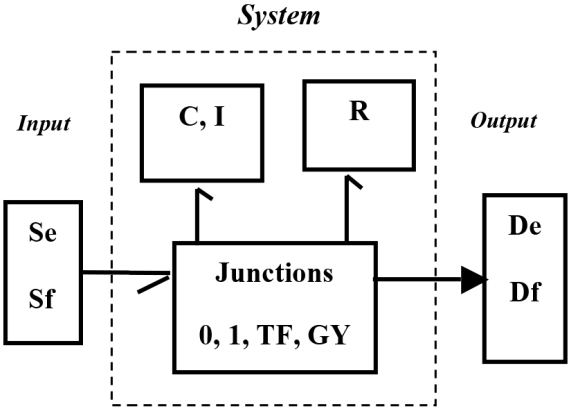

Figure 1. Diagram of the continuous system described by the bond graph.

$$\begin{cases} \dot{\hat{x}}(t) = \begin{pmatrix} \dot{\hat{p}}_I \\ \dot{\hat{q}}_c \end{pmatrix} = A \begin{pmatrix} p_L \\ q_C \end{pmatrix} + Bu(t) \\ \hat{y} = C \begin{pmatrix} \hat{p}_L \\ \hat{q}_C \end{pmatrix} \end{cases} \tag{1}$$

Figure 2 shows the basic elements of a system coupled with the Luenberger observer elements using the bond graph approach. The state equation can be written as follows:

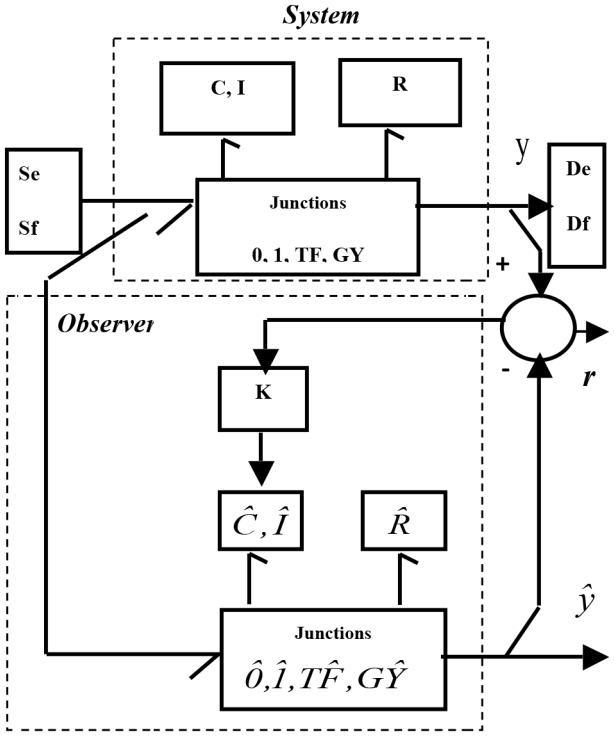

Figure 2. Structure of a Luenberger observer using the bond graph model.

$$\begin{cases} \dot{\hat{x}}(t) = \begin{pmatrix} \dot{\hat{p}}_I \\ \dot{\hat{q}}_c \end{pmatrix} = A \begin{pmatrix} p_L \\ q_C \end{pmatrix} + Bu(t) + K(y(t) - \hat{y}(t)) \\ \hat{y} = C \begin{pmatrix} \hat{p}_L \\ \hat{q}_C \end{pmatrix} \end{cases} , \tag{2}$$

where $A \begin{pmatrix} p_L \\ q_C \end{pmatrix} + Bu(t)$ is the model state equation.

$K(y(t) - \hat{y}(t))$ is the correction determined by Luenberger.

3. General description of the system

A reverse osmosis desalination water system provides fresh water from brackish or salt water (especially seawater) [25–28]. In the literature, there are several research works [29–31] interested in reverse osmosis. In this paper, our objective is determining the bond graph model of the reverse osmosis component by component in order to facilitate the detection and location of faults.

3.1. Principle of reverse osmosis

Osmosis is the solvent transfer through a membrane under the effect of a concentration gradient. If we consider a system with two compartments separated by a semiselective membrane and containing two solutions of different concentrations, osmosis results in a water flow directed from the dilute solution to the concentrated solution.

If we apply pressure on the concentrated solution, the amount of water transferred by osmosis will decrease. With a sufficiently high pressure, the water flow will even be stopped: this pressure is called the osmotic pressure P (assuming that the diluted solution is pure water). If we exceed the value of the osmotic pressure, a water flow directed oppositely to the osmotic flow is observed: this is the reverse osmosis phenomenon, as shown in Figure 3.

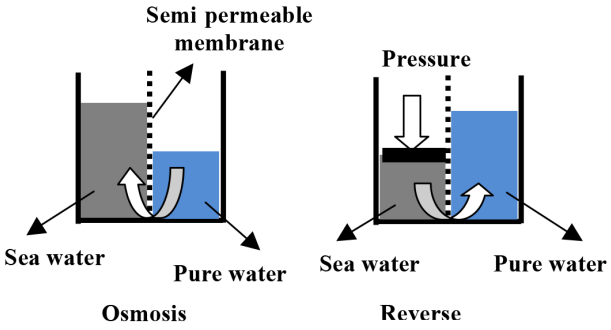

Figure 3. The phenomenon of reverse osmosis.

The osmotic pressure of the electrolyte is given by the following equation:

$$\Pi = i.C.R.T, \tag{3}$$

where i is the number of ion species constituting the solute, C the molar concentration of the solute, T the temperature, R the ideal gas constant, and Π the osmotic pressure of electrolytes. This relation is valid for dilute solutions.

3.2. Description of the test bench

The test bench (RO1500: reverse osmosis with a pump speed of 1500 rev/min) is composed of:

- A photovoltaic generator (PV) consisting of solar panels connected in series and parallel to produce the desired current and voltage for feeding the rechargeable battery pack.
- An electrical adaptation module composed of two converters, DC/DC and DC/AC, ensuring the desalination unit supply.
- A reverse osmosis desalination unit composed of two osmosis modules. Each module consists of a membrane composed of a polyamide composite thin film able to purify water of salinity less than 3g/L. Figure 4 shows the experimental system of the desalination unit.

The diagram of the test bench is given in Figure 5 and its word bond graph model is presented in Figure 6.

4. Bond graph model of the reverse osmosis

The proposed bond graph model of the reverse osmosis desalination unit is given in Figure 7. The most important parameters to be controlled are pressure P and the flow rates of produced water, Q_p, and discharged water, Q_d. The model of the reverse osmosis desalination unit is equivalent to a storage element of a hydraulic input (supply) and two outputs (water produced and rejected). It will therefore be represented in the bond graph model with a storage element (C: Cm). The flow of salt water is represented by a flow source Sf (Sf: Q_t).

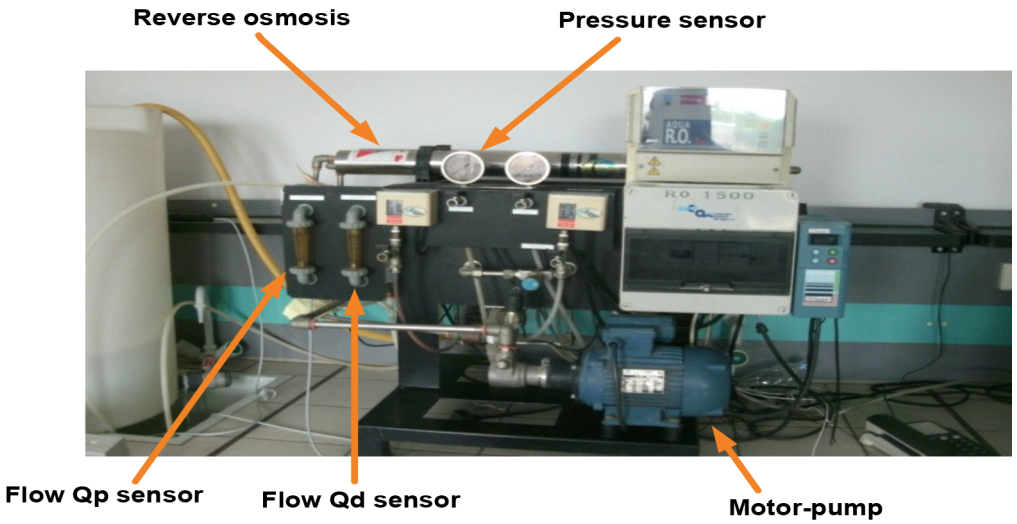

Figure 4. Experimental system of the reverse osmosis desalination unit.

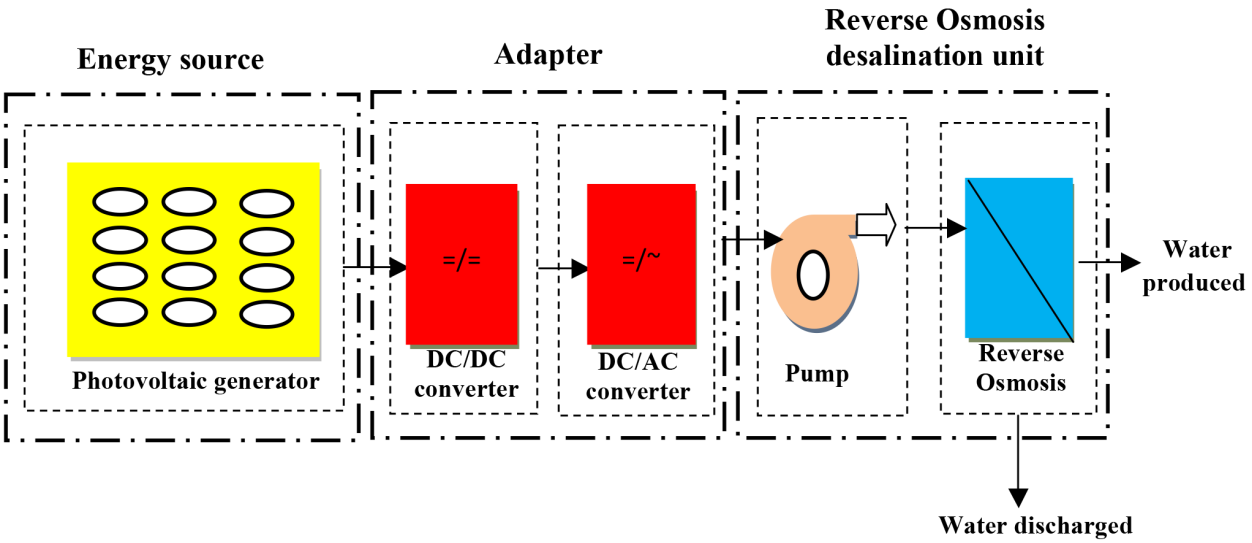

Figure 5. Test bench diagram.

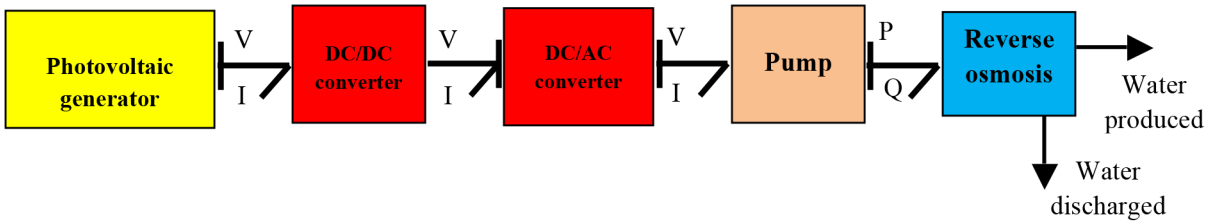

Figure 6. Word bond graph of the test bench.

(R: Rc) is the bond graph model of the pipe connecting the pump to the reverse osmosis. The membrane bond graph model is given by the element (R: Rm). The control valve is modeled by a variable resistance element (R: MR) since any change in its position causes a variation in the supply pressure; the tanks are represented by storage elements C (Cp: storing the amount of water produced, Cd: storing the amount of water discharged).

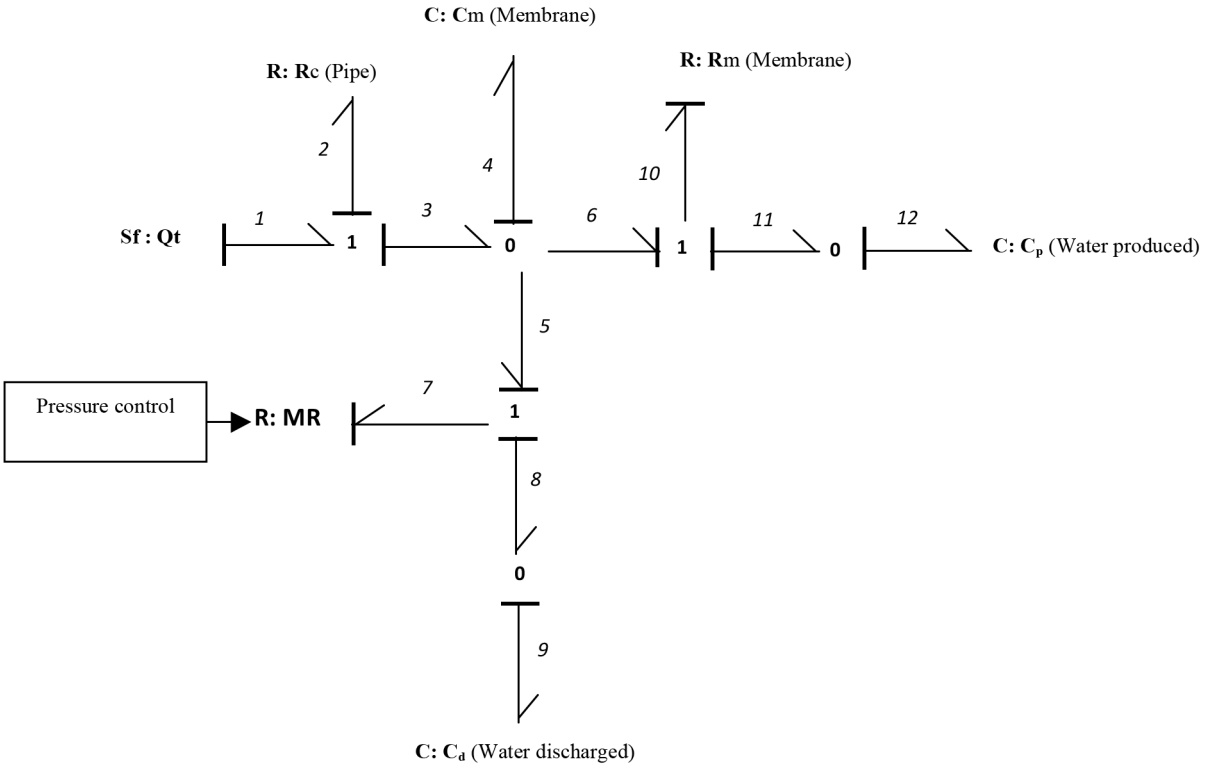

Figure 7. Bond graph model of reverse osmosis.

The 20-sim bond graph model of the reverse osmosis is given in Figure 8. This section will present the simulation and analysis of the model behavior for different values of supply pressure and discharge flows for each position of the control valve [32,33].

Figure 9 illustrates the variations of input pressure P, produced water flow Q_p, and discharged water flow Q_d as a function of each position of the control valve (MR). We notice that when the control valve is open (rejection) between instants 0 s and 50 s the supply pressure and the flow of water produced are very low, whereas when the control valve is closed for instants greater than 100 s, the flow of produced water increases while the flow of rejected water decreases.

The experimental model has three sensors for measuring pressure P_a, flow of water produced Q_p, and flow of water discharged Q_d. For each set of measurements, we manipulate these so that only one parameter (pump speed, discharge valve position) is variable while the other is kept constant. Table 1 shows the output flow rate values according to the pressure for each position of the control valve and for a rotational speed of the pump n = 1500 rev/min and salinity $C_w = 0.8$ g/L.

Curves given in Figures 10 and 11 show that when the supply pressure varies according to the control valve the flows of produced and discharged water are proportional to a constant rotational speed of the pump.

Figure 10 shows the variation of pressure P delivered by the pump and the produced water flow rate Q_p at the outlet of the reverse osmosis. We can notice that when pressure P increases flow Q_p also increases, and this is true since flow Q_p exits through the membrane; when the pressure increases, the membrane filters more water through its holes. Figure 11 shows the variation of pressure P delivered by the pump and the discharged water flow rate Q_d at the outlet of the reverse osmosis; it can be seen that the total water flow rate

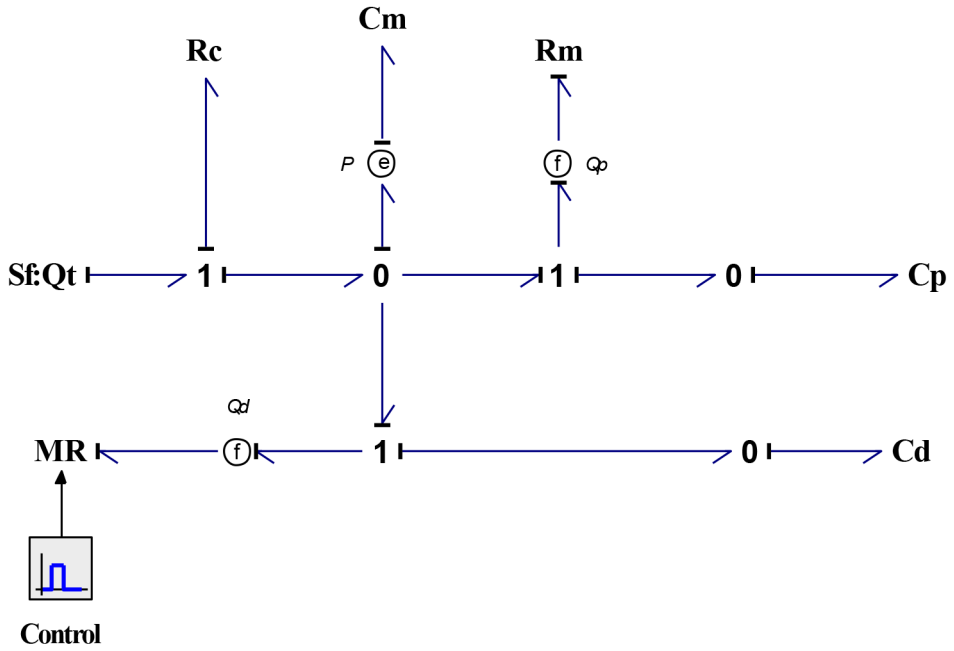

Figure 8. Bond graph model of the simulated reverse osmosis in 20-sim.

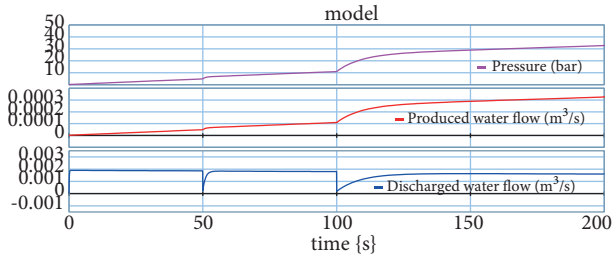

Figure 9. Variations of pressure P and produced and discharged water flows Q_p and Q_d according to the position of the control valve for n = 1500 rev/min.

Table 1. Variations of produced and discharged water flows Q_p and Q_d for each pressure P variation.

P (bar)	Q_p (m^3/s) (Experimental)	Q_p (m^3/s) (Simulated)	Q_d (m^3/s) (Experimental)	Q_d (m^3/s) (Simulated)
1	0.0018	0.0018	0.0150	0.0150
1.5	0.002	0.002	0.0145	0.0142
2	0.003	0.0028	0.0140	0.0138
2.5	0.0035	0.0032	0.0135	0.0132
3	0.0045	0.0042	0.0130	0.0128
3.5	0.0055	0.0052	0.0125	0.0122
5	0.0065	0.0062	0.0120	0.0118
6.5	0.0075	0.0072	0.0115	0.0112
7.5	0.0085	0.0082	0.0105	0.0080
8	0.009	0.0088	0.0100	0.0078

Q_t that enters the reverse osmosis is the sum of the produced and discharged water flow rates: if Q_p increases automatically Q_d decreases.

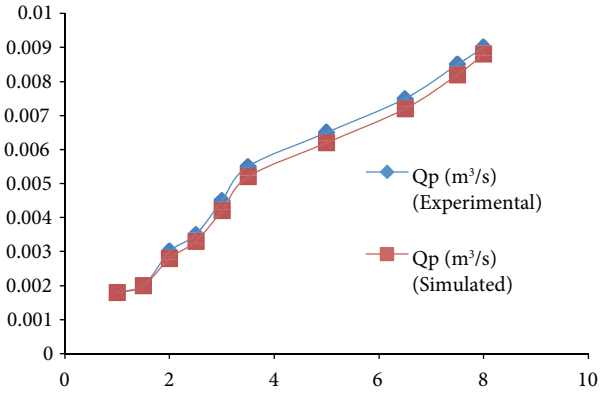

Figure 10. Variations of produced water flow Q_p for each variation of pressure P and according to the position of the control valve for n = 1500 rev/min.

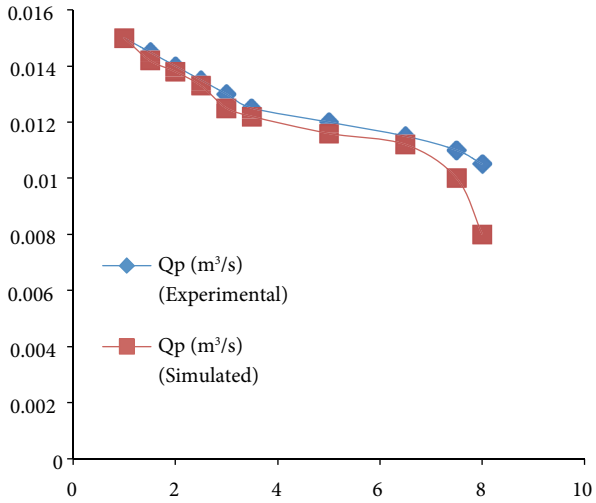

Figure 11. Variations of discharged water flow Q_d for each variation of pressure P and according to the position of the control valve for n = 1500 rev/min.

We can see from these figures that the produced water flow Q_p increases and the discharged water flow Q_d decreases with the different pressures applied to the membrane. Experimental and simulated results are similar.

5. Diagnosis of reverse osmosis

5.1. Diagnostics using the Luenberger observer based on the bond graph model

5.1.1. State equations

References [22,24] highlight the state equations with the Luenberger observer. According to the bond graph model shown in Figure 5, the state equations can be written as follows:

$$\begin{cases} \begin{pmatrix} \dot{q}_4 \\ \dot{q}_9 \\ \dot{q}_{12} \end{pmatrix} = \begin{bmatrix} -\frac{1}{C_m}\left(\frac{1}{R_m}+\frac{1}{MR}\right) & \frac{1}{C_rMR} & \frac{1}{C_pR_m} \\ \frac{1}{C_mMR} & -\frac{1}{C_rMR} & 0 \\ \frac{1}{C_mR_m} & 0 & -\frac{1}{C_pR_m} \end{bmatrix} \begin{pmatrix} q_4 \\ q_9 \\ q_{12} \end{pmatrix} + \begin{bmatrix} 1 \\ 0 \\ 0 \end{bmatrix} Q_t \\ y = \begin{bmatrix} \frac{1}{C_m} & 0 & 0 \\ \frac{1}{C_mMR} & -\frac{1}{C_rMR} & 0 \\ \frac{1}{C_mR_m} & 0 & -\frac{1}{C_pR_m} \end{bmatrix} \begin{pmatrix} q_4 \\ q_9 \\ q_{12} \end{pmatrix} \end{cases} \tag{4}$$

The reverse osmosis parameters values are summarized in Table 2.

5.1.2. Calculation of residues without faults

Figure 12 shows the construction of the Luenberger observer of the system using the bond graph approach without faults.

Table 2. Reverse osmosis parameters.

Symbol	Designation	Nominal values
Sf: Q_t	Flow source	0.02 (m^3/s)
R: r_c	Hydraulic resistance (pipe)	10 ($Pa/(m^3/s)$)
C: C_m	Hydraulic accumulator of the supply water	0.04 ($Pa/(m^3/s^2)$)
R: r_m	Hydraulic resistance (membrane)	1000 ($Pa/(m^3/s)$)
R: MR	Control valve	100 ($Pa/(m^3/s)$)
C: C_p	Produced water storage	0.02 ($Pa/(m^3/s^2)$)
C: C_d	Discharged water storage	0.004 ($Pa/(m^3/s^2)$)

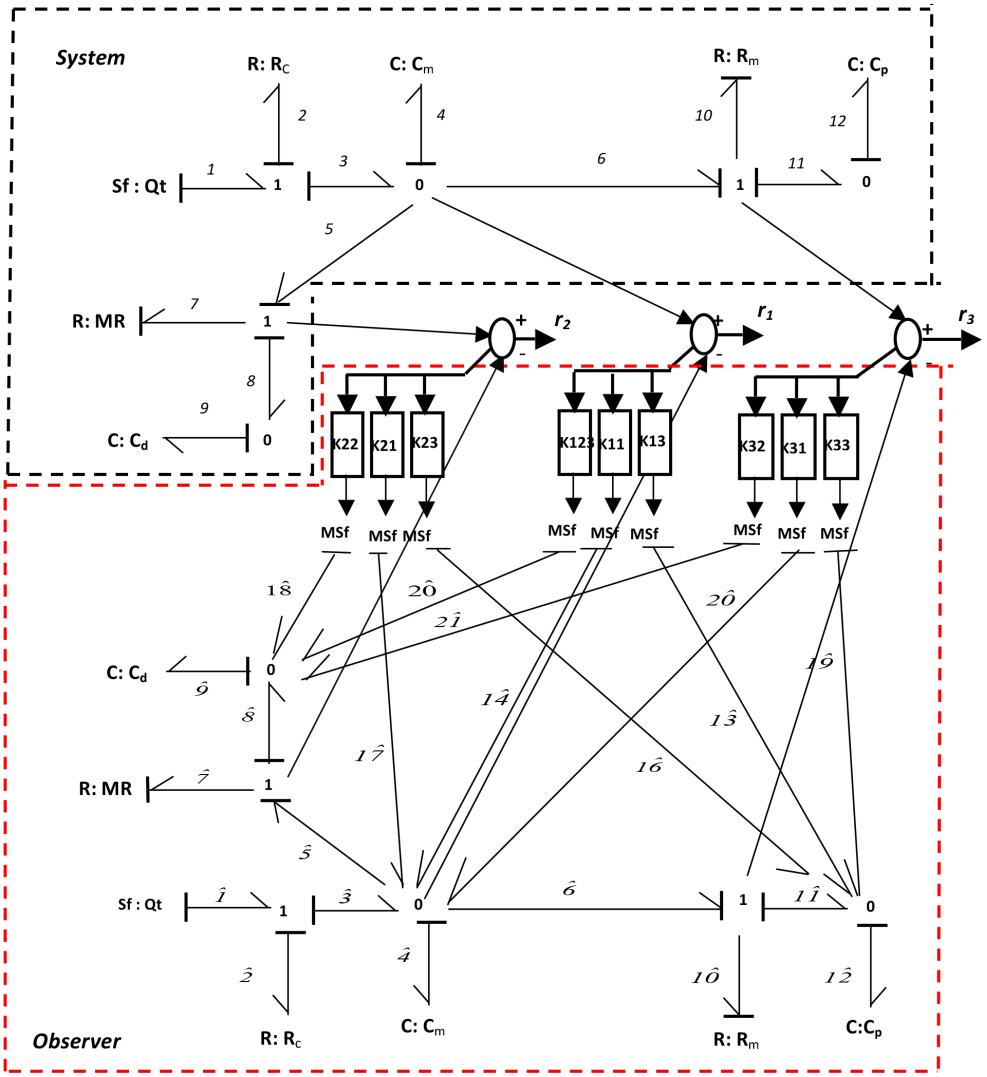

Figure 12. Luenberger observer of reverse osmosis.

After simulation in 20-sim software [34], we obtain Figure 13. Figures 13a–13c show the evolution simulation results of the system output variables with those of the observer estimated outputs. Figure 13a shows the evolution of pressure P of the system and the estimated pressure P by the Luenberger observer,

Figure 13b shows the evolution of the flow rate Q_p of the system and that estimated by the Luenberger observer, and Figure 13c shows the evolution of the flow rate Q_d of the system and that estimated by the Luenberger observer.

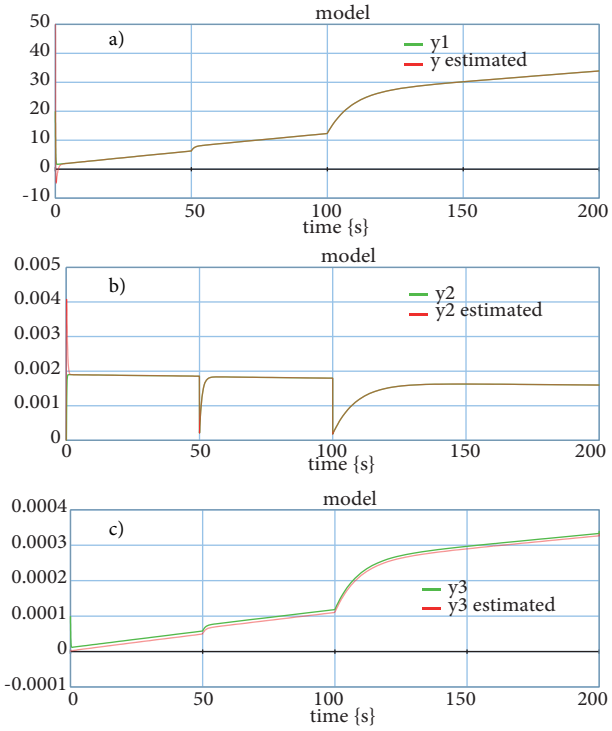

Figure 13. Estimated outputs: a) output variables y_1 and $\hat{y}_1$, b) output variables y_2 and $\hat{y}_2$, c) output variables y_3 and $\hat{y}_3$

To make the diagnosis, the residues should be calculated. From the bond graph model given in Figure 12, we can deduce residues $r_1(t)$, $r_2(t)$, and $r_3(t)$.

- Residue r_1: $e_4 - \hat{e}_4 = 0$

$$\frac{K_{12}}{C_r} r_1(t) + MR\frac{dr_2(t)}{dt} + [K_{22} - 1]\frac{1}{C_r} r_2(t) + \frac{K_{32}}{C_r} r_3(t) = 0 \tag{5}$$

- Residue r_2: $f_7 - \hat{f}_7 = 0$

$$\begin{aligned} &-(C_m + C_p)\tfrac{dr_1(t)}{dt} + C_p R_m \tfrac{dr_3(t)}{dt} - (K_{11} + K_{13}) r_1(t) - (K_{21} + K_{23}) r_2(t) \\ &-(K_{31} + K_{33}) r_3(t) = 0 \end{aligned} \tag{6}$$

- Residue r_3: $f_{10} - \hat{f}_{10} = 0$

$$\begin{aligned} &-(C_m + C_r)\tfrac{dr_1(t)}{dt} + C_r MR \tfrac{dr_2(t)}{dt} - (K_{11} + K_{12}) r_1(t) - (K_{21} + K_{22}) r_2(t) \\ &-(K_{31} + K_{32}) r_3(t) = 0 \end{aligned} \tag{7}$$

Figure 14 shows that the residues converge to zero.

5.1.3. Generation of residues with sensors faults

Sensors De, Df_1, and Df_2 are affected respectively by faults F_{C1}, F_{C2}, and F_{C3}, and then:

- Residue r_1: $(e_4 + F_{C1}) - \hat{e}_4 = 0$

$$\frac{K_{12}}{C_r} r_1(t) + MR\frac{dr_2(t)}{dt} + [K_{22} - 1]\frac{1}{C_r} r_2(t) + \frac{K_{32}}{C_r} r_3(t) + \frac{dF_{C1}(t)}{dt} - MR\frac{dF_{C2}(t)}{dt} - \frac{1}{C_r} F_{C2}(t) = 0 \quad (8)$$

- Residue r_2: $(f_7 + F_{C2}) - \hat{f}_7 = 0$

$$-K_{11} r_1(t) - C_m \cdot \frac{dr_1(t)}{dt} - K_{21} r_2(t) - (1 + K_{31}) r_3(t) - F_{C1}(t) + F_{C2}(t) - F_{C3}(t) = 0 \quad (9)$$

- Residue r_3: $(f_{10} + F_{C3}) - \hat{f}_{10} = 0$

$$-K_{11} r_1(t) - C_m \frac{dr_1(t)}{dt} - (K_{21} + 1) r_2(t) - K_{31} r_3(t) - F_{C1}(t) - F_{C2}(t) + F_{C3}(t) = 0 \quad (10)$$

Eqs. (8), (9), and (10) show that $r_1(t)$, $r_2(t)$, and $r_3(t)$ are sensitive to the De, Df_1, and Df_2 sensors faults; Figure 15 confirms this.

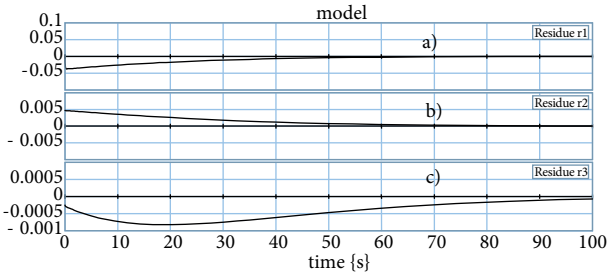

Figure 14. Residues $r_1(t)$, $r_2(t)$, and $r_3(t)$ in the case of normal operation.

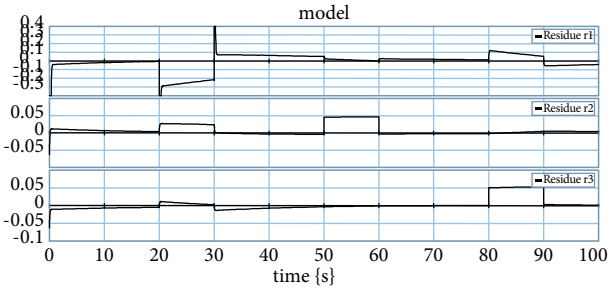

Figure 15. Residues $r_1(t)$, $r_2(t)$, and $r_3(t)$ with sensors faults.

We can notice that all residues are sensitive to each fault sensor and this is confirmed by the equations established previously. It may be possible to use the dedicated observer scheme and generalized observer scheme structures to locate faults. This is left as future work.

6. Conclusion

In this paper, we have proposed a new methodology for supervising industrial systems. Our contribution is the development of a supervision strategy based on a proportional observer (Luenberger observer) for linear systems using bond graph models.

The bond graph model is used for modeling and determining residues with the Luenberger observer. Indeed, complete knowledge of the system state is often required in developing a control law or the establishment of a surveillance or diagnostic strategy. However, the state of a system is generally only partially available and the input and output signals are in practice the only variables accessible by measurement. The most common solution to overcome this problem is to combine the existing system with an auxiliary system known as an estimator or state observer. The observer provides an estimate of the system state from the model and measurements of its inputs and outputs. Furthermore, we have exploited the architectural aspect of the bond

graph representation of industrial systems in the diagnostic condition based on Luenberger observers. We have also shown how to use a bond graph approach for modeling, state estimation, fault detection, and simulation of dynamical systems. The research was based on 20-sim software, which allowed us to build the system and the Luenberger observer in a simple way since the bond graph approach models the system and the Luenberger observer component by component. This kind of modeling facilitated the detection and localization of faults.

Nomenclature

C Molar concentration of the solute
C_d Discharged water storage
C_m Hydraulic accumulator of the supply water
C_p Produced water storage
C_w Water salinity
D_e Effort sensor
F_{Ci} Fault
i Number of ion species constituting the solute
Qd Flow of discharged water
Qp Flow of produced water
Qt Total water flow rate
ri Residue
Rc Hydraulic resistance (pipe)
Rm Hydraulic resistance (membrane)
T Temperature
Π Osmotic pressure of electrolytes

References

[1] Luenberger D. Observers for multivariable systems. IEEE T Automat Contr 1966; 11: 190-197.

[2] Guerra RM, Luviano-Juárez A, Rincón-Pasaye JJ. Fault estimation using algebraic observers. In: Proceedings of the 2007 American Control Conference; 11–13 July 2007; New York City, NY, USA. pp. 438-442.

[3] Baffet G, Charara A, Lechner D. Estimation of vehicle side slip, tire force and wheel cornering stiffness. Cont Eng Pract 2009; 17: 1255-1264.

[4] Stéphant J, Charara A, Meizel D. Evaluation of a sliding mode observer for vehicle side slip angle. Cont Eng Pract 2007; 15: 803-812.

[5] Paynter HM. Analysis and Design of Engineering Systems. Boston, MA, USA: MIT Press, 1961.

[6] Khedher A, Othman KB, Benrejeb M, Maquin D. Adaptive observer for fault estimation in nonlinear systems described by a Takagi-Sugeno model. In: 18th Mediterranean Conference on Control and Automation; 23–25 June 2010; Marrakech, Morocco. pp. 261-266.

[7] Karnopp D, Margolis D, Rosenberg R. System Dynamics: A Unified Approach. New York, NY, USA: Wiley, 1990.

[8] Dauphin-Tanguy G. Les bond graphs. Paris, France: Hermes Science Publications, 2000 (in French).

[9] Ould Bouamama B, Dauphin-Tanguy G. Bond graph modelling: Base elements for energetics. Paris, France: Techniques de l'ingénieur, 2006.

[10] Frih A, Chalh Z, Mrabti M, Ouahi M, Alfidi M. La conception d'observateur d'un système mécanique dans le domaine d'automobile par l'approche graphique. In: Xème Conférence Internationale: Conception et Production Intégrées; December 2015; Tangier, Morocco (in French).

[11] Chalh Z, Frih A, Mrabti M, Alfidi M. Bond graph methodology for controllability of LTV systems International Journal of Modelling, Identification and Control 2015; 24: 257-265.

[12] Tagina M. Application de la modélisation bond graph à la surveillance des systèmes complexes. PhD, Lille University, Lille, France, 1995 (in French).

[13] Azmani A, Dauphin-Tanguy G. ARCHER: A program for computer aided modelling and analysis. In: Dauphin-Tanguy G, Breedveld P, editors. Bond Graphs for Engineers. Amsterdam, the Netherlands: Elsevier, 1992. pp. 263-278.

[14] Karnopp D. Bond graphs in control: physical state variables and observers. J Franklin Inst 1979; 308: 221-234.

[15] Costello DJ, Gawthrop P. Physical model-based control: experiments with a stirred-tank heater. Chem Eng Res Des 1997; 75: 361-370.

[16] Gawthrop PJ, Smith LPS. Metamodelling: Bond Graphs and Dynamic Systems. London, UK: Prentice Hall International, 1996.

[17] Roberts DW, Ballance DJ, Gawthrop PJ. Design and implementation of a bond graph observer for robot control. Cont Eng Pract 1995; 3: 1447-1457.

[18] Sueur C, Dauphin-Tanguy G. Bond graph approach for structural analysis of MIMO linear systems. J Franklin Inst 1991; 328: 55-70.

[19] Pichardo-Almarza C, Rahmani A, Dauphin-Tanguy G, Delgado M. Bond graph approach to build reduced order observers in linear time invariant systems. In: Proceedings of the 4th MATHMOD International Symposium on Mathematical Modelling; 2003.

[20] Pichardo-Almarza C, Rahmani A, Dauphin-Tanguy G, Delgado M. High gain observers for nonlinear systems modelled by bond graphs. P I Mech Eng I-J Sys 2005; 219: 477-498.

[21] Pichardo-Almarza C, Rahmani A, Dauphin-Tanguy G, Delgado M. Luenberger observers for linear time invariant systems modelled by bond graph. Math Comp Model Dyn 2006; 12: 219-234.

[22] Luenberger D. An introduction to observers. IEEE T Automat Contr 1971; 16: 596-602.

[23] Ouahi M, Stéphant J, Meizel D. Redefining automotive supervision using new sensor technology. In: Proceedings of the International Symposium on Advanced Vehicle Control; August 2010; Loughborough, UK.

[24] Marino R, Scalzi S. Asymptotic sideslip angle and yaw rate decoupling control in four-wheel steering vehicles. Veh Syst Dyn 2010; 48: 999-1019.

[25] Merten U. Desalination by Reverse Osmosis. Cambridge, MA, USA: MIT Press, 1966.

[26] Rautenbach R, Albercht R. Membrane Processes. 1st ed. Oxford, UK: Wiley, 1989.

[27] Lacey RE, Loeb S. Industrial Processing with Membranes. New York, NY, USA: Wiley-Interscience, 1972.

[28] Sourirajan S. Reverse osmosis: a new field of applied chemistry and chemical engineering. In: ACS Symposium Series (USA); 1981. pp. 153-154.

[29] Bartman AR, Christofides PD, Cohen Y. Nonlinear model-based control of an experimental reverse-osmosis water desalination system. Ind Eng Chem Res 2009; 48: 6126-6136.

[30] Laborde HM, França KB, Neff H, Lima AMN. Optimization strategy for a small-scale reverse osmosis water desalination system based on solar energy. Desalination 2001; 133: 1-12.

[31] Mokheimer EMA, Sahin AZ, Al-Sharafi A, Ali AI. Modeling and optimization of hybrid wind–solar-powered reverse osmosis water desalination system in Saudi Arabia. Energy Convers Manage 2013; 75: 86-97.

[32] Robertson MW, Watters JC, Desphande PB, Assef JZ, Alatiqui I. Model based control for reverse osmosis desalination processes. Desalination 1996; 104: 59-68.

[33] Mandler JA. Modelling for control analysis and design in complex industrial separation and liquefaction processes. J Proc Cont 2000; 10: 167-175.

[34] Broenink JF. 20-sim software for hierarchical bond-graph/block-diagram models. Sim Pract Theory 1999; 7: 481-492.